Observational aspects of weak lensing

Overview

- Shape measurement
- Photometric redshifts
- Intrinsic alignment
- Non-linear structure formation
- Non-Gaussian errors

(Leiden list)

Measuring ellipticity

Reminder:
Weak gravitational lensing causes small image distortions.
(Linearized) lens mapping: circle → ellipse.

Need to measure "ellipticity" for irregular shaped objects such as faint, high-redshift galaxies...

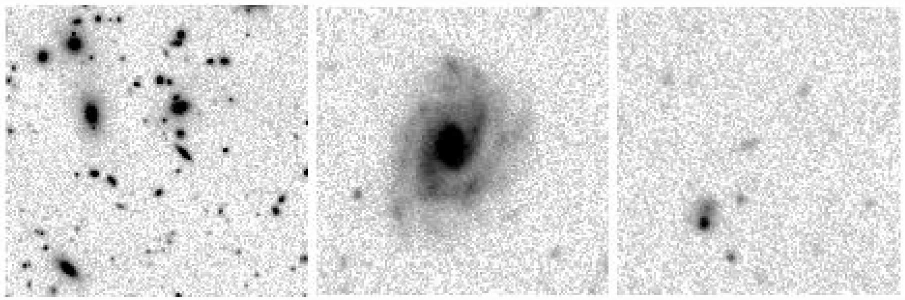

[Y. Mellier]

Defining ellipticity

- Second-order tensor of brightness distribution

$$Q_{ij} = \frac{\int \mathrm{d}^2\theta \, q[I(\boldsymbol{\theta})] \, (\theta_i - \bar{\theta}_i)(\theta_j - \bar{\theta}_j)}{\int \mathrm{d}^2 \, \theta \, q[I(\boldsymbol{\theta})]}, \quad i, j = 1, 2$$

$I(\boldsymbol{\theta})$: brightness distribution of galaxy

q : weight function

$$\bar{\boldsymbol{\theta}} = \frac{\int \mathrm{d}^2\theta \, q_I[I(\boldsymbol{\theta})] \, \boldsymbol{\theta}}{\int \mathrm{d}^2\theta \, q_I[I(\boldsymbol{\theta})]} : \quad \text{barycenter}$$

- Ellipticity

$$\varepsilon = \frac{Q_{11} - Q_{22} + 2\mathrm{i}Q_{12}}{Q_{11} + Q_{22} + 2(Q_{11}Q_{22} - Q_{12}^2)^{1/2}}$$

- Circular object $Q_{11} = Q_{22}, Q_{12} = Q_{21} = 0$
- Elliptical isophotes, axis ratio r: $|\varepsilon| = (1 - r)/(1 + r)$

From source to image

- Analogously define $Q^{\rm s}_{ij}$ for source brightness
- With lens equation:

$$Q^{\rm s} = \mathcal{A} Q \mathcal{A}$$

[Reminder:

$$\mathcal{A} = \begin{pmatrix} 1-\kappa-\gamma_1 & -\gamma_2 \\ -\gamma_2 & 1-\kappa+\gamma_1 \end{pmatrix} = (1-\kappa) \begin{pmatrix} 1-g_1 & -g_2 \\ -g_2 & 1+g_1 \end{pmatrix}$$

Jacobi-matrix of mapping between lens and source position. Reduced shear $g_i = \gamma_i/(1-\kappa)$]

- Relation between source $\varepsilon^{\rm s}$ and image ellipticity ε

$$\varepsilon^{\rm s} = \begin{cases} \dfrac{\varepsilon - g}{1 - g^* \varepsilon} & \text{for} \quad |g| \le 1 \\[2ex] \dfrac{1 - g\varepsilon^*}{\varepsilon^* - g^*} & \text{for} \quad |g| > 1 \end{cases},$$

- weak-lensing regime: $\kappa, |\gamma| \ll 1 \rightarrow \varepsilon \approx \varepsilon^{\rm s} + \gamma$

Measuring second-order shear

Estimators

- 2PCF: correlate all galaxy pairs

$$\hat{\xi}_{\pm}(\vartheta) = \frac{1}{N_{\rm pair}} \sum_{\substack{ij \\ \text{pairs} \in \vartheta-\text{bin}}}^{N_{\rm pair}} \left(\varepsilon_{i{\rm t}} \varepsilon_{j{\rm t}} \pm \varepsilon_{i\times} \varepsilon_{j\times} \right)$$

- Aperture-mass dispersion: place apertures over data field

$$\hat{M}(\theta) = \frac{1}{N_{\rm ap}} \sum_{n=1}^{N_{\rm ap}} \frac{1}{N_n(N_n - 1)} \sum_{\substack{i \neq j \\ \text{gal} \in \text{ap.}}}^{N_n} Q_i Q_j \varepsilon_{i{\rm t}} \varepsilon^*_{j{\rm t}}$$

(tophat-variance similar)

Interrelations

Placing apertures very inefficient due to gaps, masking. Correlating pairs for 2PCF makes optimal use of data.

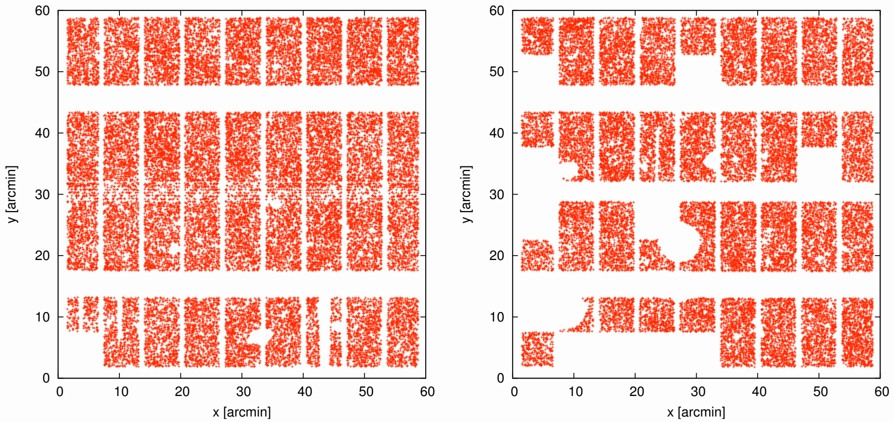

Invert relation between 2PCF and power spectrum $\longrightarrow$ express aperture measures in terms of 2PCF

Interrelations

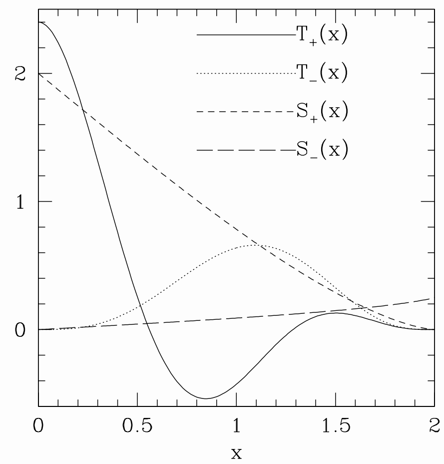

$T_\pm, S_\pm$ depend on $\hat{U}$, analytical expressions exist

$$\langle M_{\rm ap}^2\rangle(\theta) = \int_0^{2\theta} \frac{{\rm d}\vartheta\,\vartheta}{\theta^2}\, T_+\left(\frac{\vartheta}{\theta}\right) \xi_+(\vartheta)$$
$$= \int_0^{2\theta} \frac{{\rm d}\vartheta\,\vartheta}{\theta^2}\, T_-\left(\frac{\vartheta}{\theta}\right) \xi_-(\vartheta)$$

$$\langle |\gamma|^2\rangle(\theta) = \int_0^{2\theta} \frac{{\rm d}\vartheta\,\vartheta}{\theta^2}\, S_+\left(\frac{\vartheta}{\theta}\right) \xi_+(\vartheta)$$
$$= \int_0^{\infty} \frac{{\rm d}\vartheta\,\vartheta}{\theta^2}\, S_-\left(\frac{\vartheta}{\theta}\right) \xi_-(\vartheta)$$

Interrelations in the presence of a B-mode

$$\langle M^2_{\mathrm{ap},\times}\rangle(\theta) = \frac{1}{2}\left[\int_0^{2\theta} \frac{\mathrm{d}\vartheta\,\vartheta}{\theta^2}\, T_+\left(\frac{\vartheta}{\theta}\right)\xi_+(\vartheta) \;\pm\; \int_0^{2\theta} \frac{\mathrm{d}\vartheta\,\vartheta}{\theta^2}\, T_-\left(\frac{\vartheta}{\theta}\right)\xi_-(\vartheta)\right]$$

$$\langle|\gamma|^2\rangle_{\mathrm{E,B}}(\theta) = \frac{1}{2}\left[\int_0^{2\theta} \frac{\mathrm{d}\vartheta\,\vartheta}{\theta^2}\, S_+\left(\frac{\vartheta}{\theta}\right)\xi_+(\vartheta) \;\pm\; \int_0^{\infty} \frac{\mathrm{d}\vartheta\,\vartheta}{\theta^2}\, S_-\left(\frac{\vartheta}{\theta}\right)\xi_-(\vartheta)\right]$$

$$\xi_{\mathrm{E,B}}(\theta) = \frac{1}{2}\left[\xi_+(\theta) \;\pm\; \xi_-(\theta) \pm \int_\theta^\infty \frac{\mathrm{d}\vartheta}{\vartheta}\xi_-(\vartheta)\left(4 - 12\frac{\theta^2}{\vartheta^2}\right)\right]$$

Top-hat-variance and corr. function not local!

E- and B-mode mixing

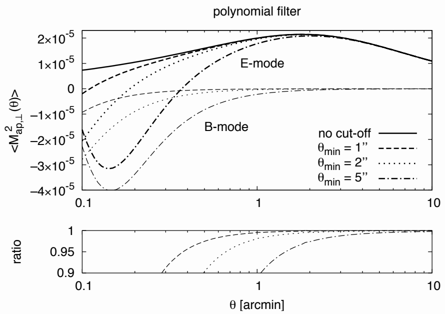

Aperture-mass statistics: B-mode on small scales due to minimum angular scales (blending of galaxy images)

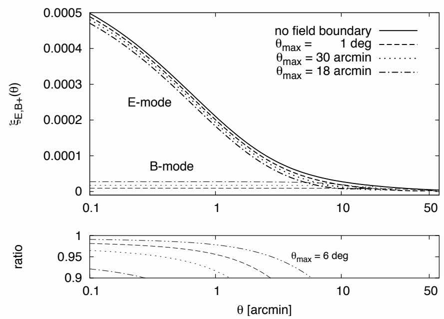

Correlation function and top-hat-variance: ≈ constant B-mode on all scales due to maximum scale (field size)

[MK, Schneider & Eifler 2006]

E-/B-mode separation on finite angular range: Ring statistics

[Schneider & MK 2006]

PSF effects

The problem:

- Need to measure galaxy shapes to percent-level accuracy.
- Galaxies are faint ($I > 21$), small ($\gtrsim$ arcsec = few pixel) and are
    1. smeared by seeing
    2. distorted by instrumental imperfections: defocusing, abberation, coma etc., tracking errors, chip not planar, image coaddition

  Effect:
    1. Makes galaxies rounder
    2. Mimics a shear signal $\gg \gamma$!

  Solution:
    1. Seeing $\lesssim 1''$
    2. Correct for PSF anisotropies

Example of star images

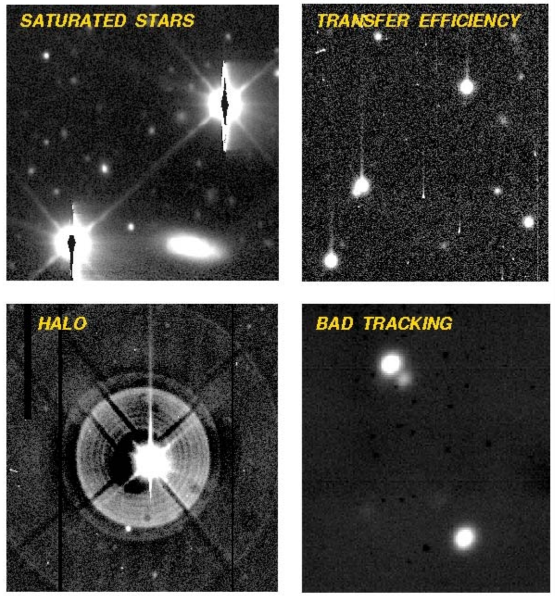

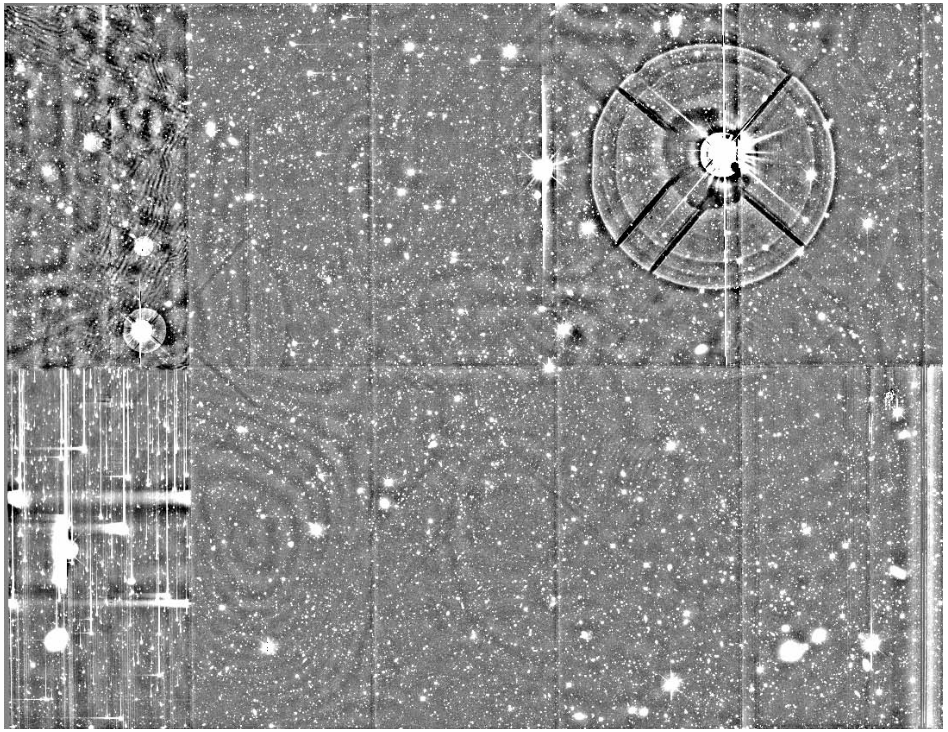

KSB

[Kaiser, Squires & Broadhurst 1995]: Perturbative ansatz for PSF effects

$$\varepsilon^{\rm obs} = \varepsilon^{\rm s} + P^{\rm sm}\varepsilon^* + P^{\rm sh}\gamma$$

[c.f. $\varepsilon^{\rm obs} = \varepsilon^{\rm s} + \gamma$ from before]

$P^{\rm sm}$	smear polarisability, (linear) response of to ellipticity to PSF anisotropy
e^*	PSF anisotropy
$P^{\rm sh}$	shear polarisability, isotropic seeing correction
γ	shear

$P^{\rm sm}, P^{\rm sh}$ are functions of galaxy brightness distribution.
e^*: fit function (polynomial/rational) to star PSFs, extrapolate to galaxy positions

PSF effects depend on galaxy . . .

- size
- magnitude
- morphology
- SED (color gradient within broad-band filter)

Object selection

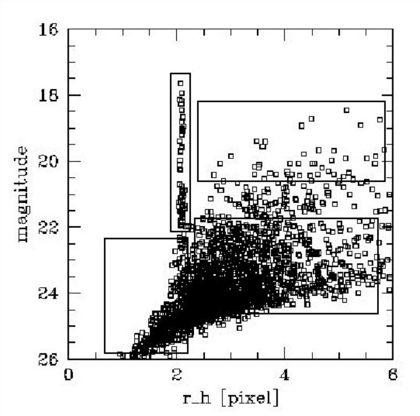

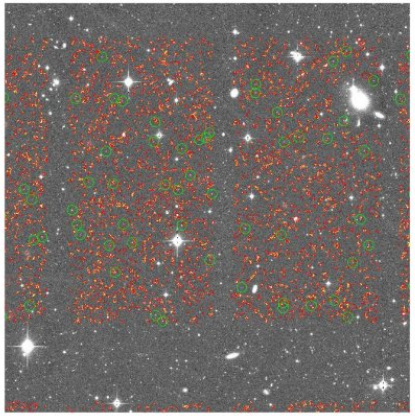

CFHTLS Wide [I. Tereno]

From size-magnitude diagram select galaxies and stars.

PSF pattern

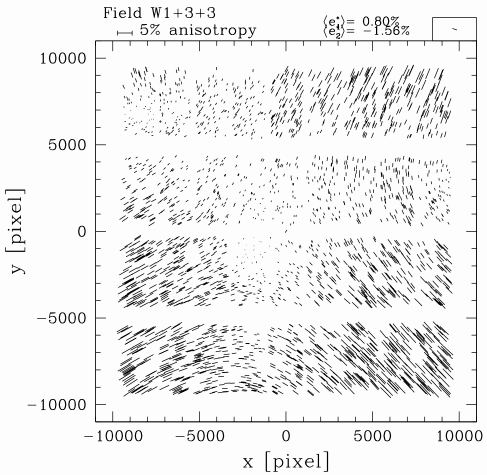

PSF correction works if

- PSF pattern is smooth (can be fitted by simple function)
- star density is high enough (∼ 10-20 stars per chip)

[Hoekstra et al. 2006]

PSF correction

55 CFHTLS Wide pointings

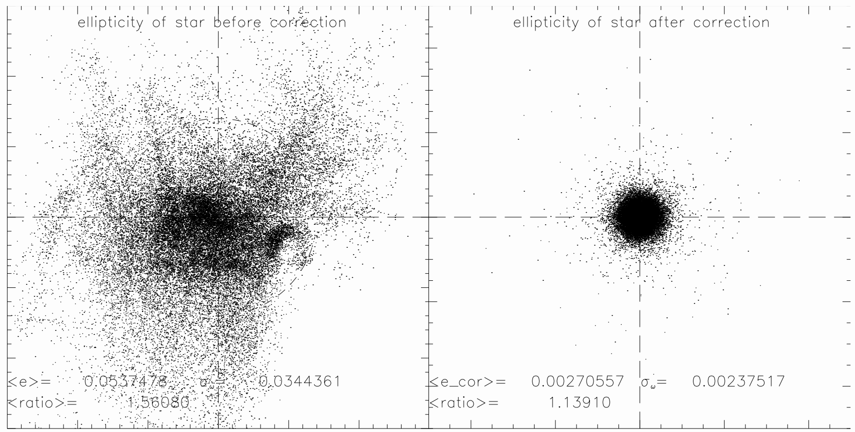

[Fu et al. 2007 (in prep.)]

KSB alternatives

Shapelets [Refregier 2003, Massey & Refregier 2003, Kuijken 2006]

- Decompose galaxies and stars into basis functions.

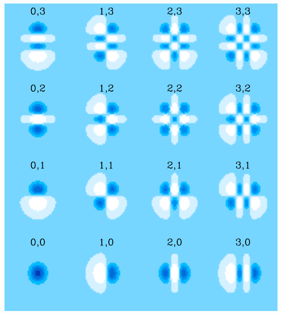

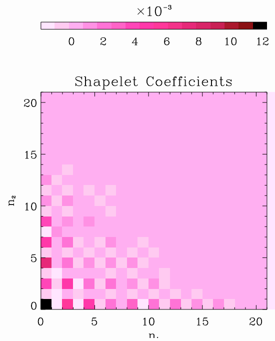

- PSF correction, convergence and shear acts on shapelet coefficients, deconvolution feasible
- Beyond second-order (quadrupole moment)

KSB alternatives

PCA decomposition [Bernstein & Jarvis 2002, Nakajima & Bernstein 2007]

Similar to shapelets method, but shears the basis functions until they match observed galaxy image

im2shape [Kuijken 1999, Bridle et al. 2002]

Fits sum of elliptical Gaussian to each galaxy (MCMC). In principle offers clean way to translate shape measurement errors into errors on cosmological parameters. But: Very slow!

Weak lensing from space

Advantages and disadvantages

- No seeing, resolution is diffraction-limited (HST: < 100 mas)
- Deeper (higher z, larger number density), better IR-coverage than from earth
- HST: PSF undersampled, 'ugly', time-variations
- small field of view, few stars
- CCD 'aging', many cosmic rays, CTE problems

Results

- Cluster WL: excellent results (high shear signal, calibration less crucial)
- Cosmic shear: COSMOS, GEMS, GOODS, ACS parallel survey

Space-based cosmic shear surveys

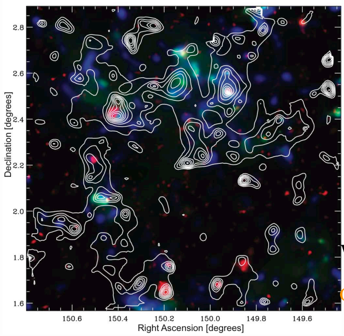

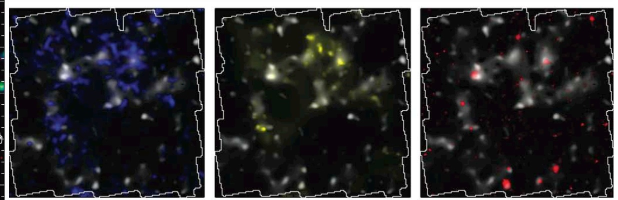

WL mass (contours), stellar mass, galaxy density, X-ray

[Massey et al. 2007]

STEP = Shear TEsting Programme

- World-wide collaboration of most of the weak lensing groups, started in 2004.
- Blind analysis of simulated images to test and calibrate different shape measurement methods, data reduction pipelines.

STEP 1	Simple Galaxy and PSF types	Heymans et al. 2006
STEP 2	Galaxy images with shapelets	
	Results from STEP 1 used	Massey et al. 2007
STEP 3	Space-based observations	in prep.
STEP 4	Back to the roots?	

...

STEP results

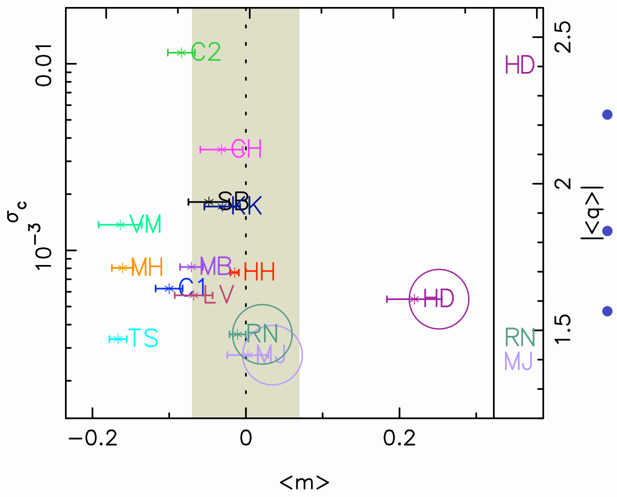

- Multiplicative m and additive errors σ_c, $\gamma^{\rm obs} - \gamma^{\rm true} = m\gamma^{\rm true} + c$
- Best methods measure better shear than 7%
- STEP 2: Sub-percent level not yet reached

Principle of photo-zs

- Redshifted galaxy spectra have different colors

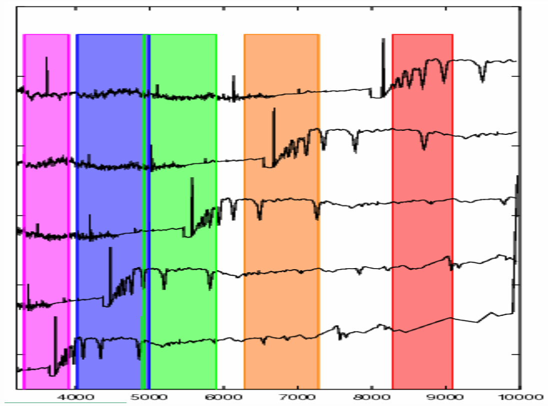

[from Y. Mellier]

- 4000 Å-break strongest feature → ellipticals (old stellar population) best, spirals ok, irregular/star-burst (emission lines) very unreliable

Photometric redshifts

- Redshift desert $z \approx 1.5 - 2.5$, neither 4000 Å-break nor Ly-break in visible range
- Confusion between low-z dwarf ellipticals and high-z galaxies
- Need UV band and IR for high redshifts! But: UV very insensitive, IR absorbed by atmosphere, have go to space
- Need database of galaxy spectra templates (observed or synthetic)
- Calibrate with spectroscopic galaxy sample. But always $N_{\rm spec} \ll N_{\rm WL}$

Photo-z calibration

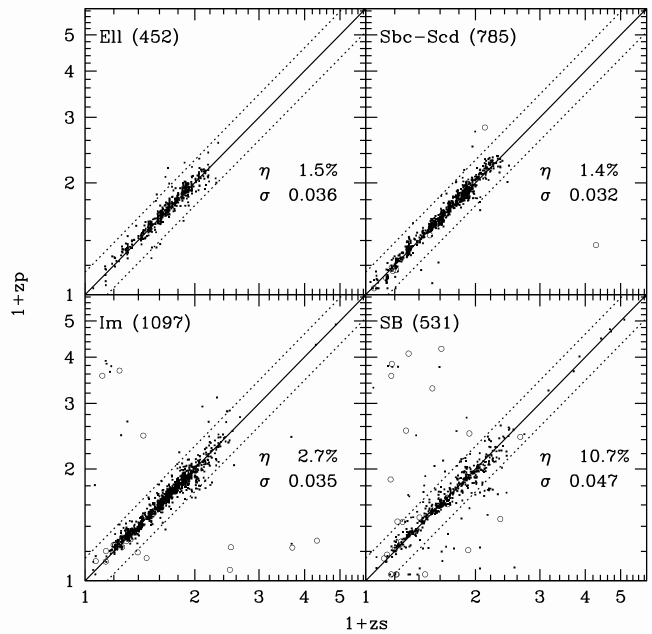

Minimize catastrophic failures

$$\frac{z_{\rm ph} - z}{1+z} \lesssim 0.5$$

$17.5 \leq i'_{AB} \leq 24$

[Ilbert et al. 2006]

Photometric errors and cosmology

Degradation of w_a-constraint as fct. of uncertainty in photo-z parameters $\Delta z_{\rm bias} = \Delta\sigma_z$

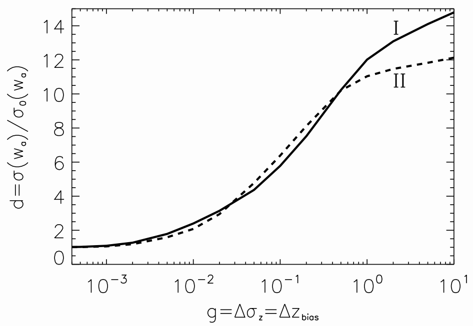

perfect redshifts:

$\sigma_0(w_a)$ =0.69 (I)

$\sigma_0(w_a)$ =0.96 (II)

Cumulative number of galaxies in spectroscopic sample for degradation = 1.5

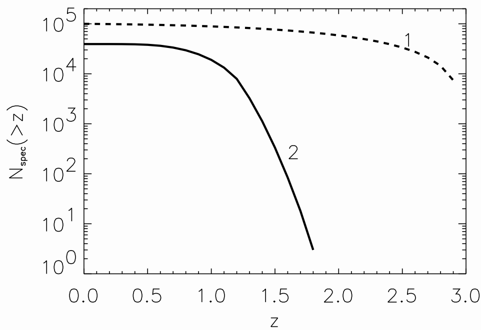

[Ma, Hu & Huterer 2006]

Size of spectroscopic sample

Error on bias and dispersion in μ^{th} redshift bins

$$\Delta z^{\mu}_{\text{bias}} = \frac{\sigma^{\mu}_{z}(\text{ind. gal})}{\sqrt{N^{\mu}_{\text{spect}}}}$$

$$\Delta \sigma^{\mu}_{z} = \frac{\sigma^{\mu}_{z}(\text{ind. gal})}{\sqrt{N^{\mu}_{\text{spect}}/2}}$$

Assume $\sigma_z(\text{ind. gal}) = 0.1$, 5 photo-z bands. To reach $\Delta z^{\mu}_{\text{bias}} = 10^{-3}$, we need a total of $N_{\text{spec}} = 5 \cdot 10^4$ spectra!

Requirements for high-precision cosmology

- some 10^4 spectra to very faint magnitudes
- IR bands from space

Other possibilities

- Intermediate calibration step between ≈ 5 bands and spectra: large number of broad bands from UV to far-IR (10^3 spectra sufficient?)
- Angular correlation between photo-z bins to determine true z-distribution (e.g. correlation between low- and high-z bins $\leftarrow$ contamination by catastrophic outliers)

Intrinsic alignment

Intrinsic-intrinsic correlation (II)

- Reminder: basic equation of weak lensing $\varepsilon = \varepsilon^{\mathrm{s}} + \gamma$
- Second-order correlations

$$\langle \varepsilon_i \varepsilon_j^* \rangle = \langle \varepsilon_i^{\mathrm{s}} \varepsilon_j^{\mathrm{s}*} \rangle + \langle \varepsilon_i^{\mathrm{s}} \gamma_j^* \rangle + \langle \gamma_j \varepsilon_j^{\mathrm{s}*} \rangle + \langle \gamma_i \gamma_j^* \rangle$$

- $\langle \varepsilon_i^{\mathrm{s}} \varepsilon_j^{\mathrm{s}*} \rangle \neq 0$ for $z_i \approx z_j$, and if shapes of galaxies intrinsically correlated, e.g. through spin-coupling with dm halo, tidal torques
- II measured in COMBO-17 (Heymans et al. 2004), not measured in SDSS (Hirata et al. 2004). B-modes as diagnostics?
- Theoretical predictions do not agree with each other

Theoretical predictions of II-correlation

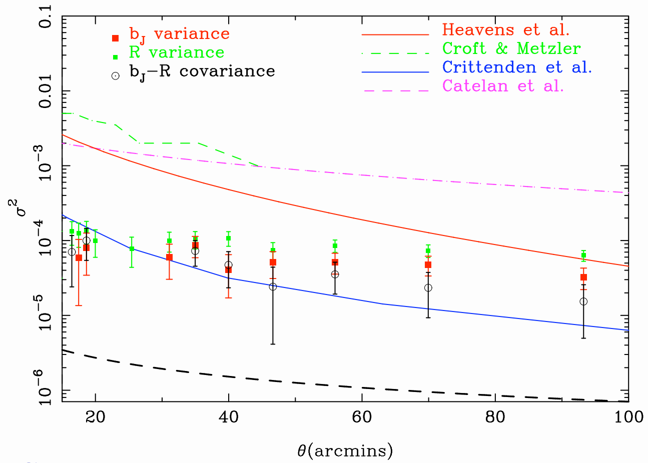

[Brown et al. 2002]

Conclusion

- II-contamination probably unimportant. Can be reduced by going deep, and down-weighting (physically) close pairs (photo-zs!)

Intrinsic-shear correlation (GI)

- $\langle \varepsilon_i^{\rm s} \gamma_j^* \rangle \neq 0$ for $z_i < z_j$, and if foreground galaxy aligned with its halo that causes lensing signal

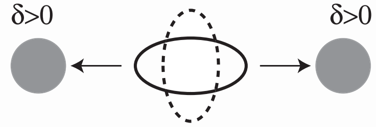

mass quadrupole

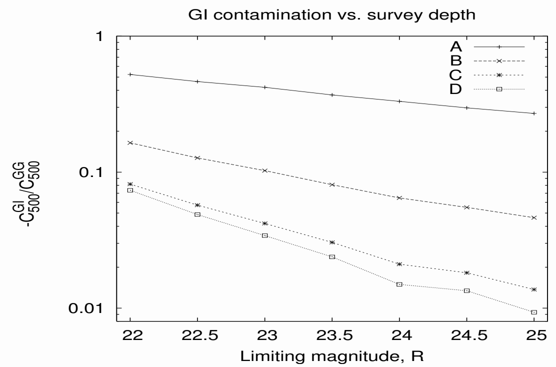

- Anti-correlation between background shear and foreground orientation → underestimate σ_8 by up to 10%
- Unlike II, GI cannot be down-weighted!

[Hirata et al. 2004, 2007] SDSS+2SLAQ

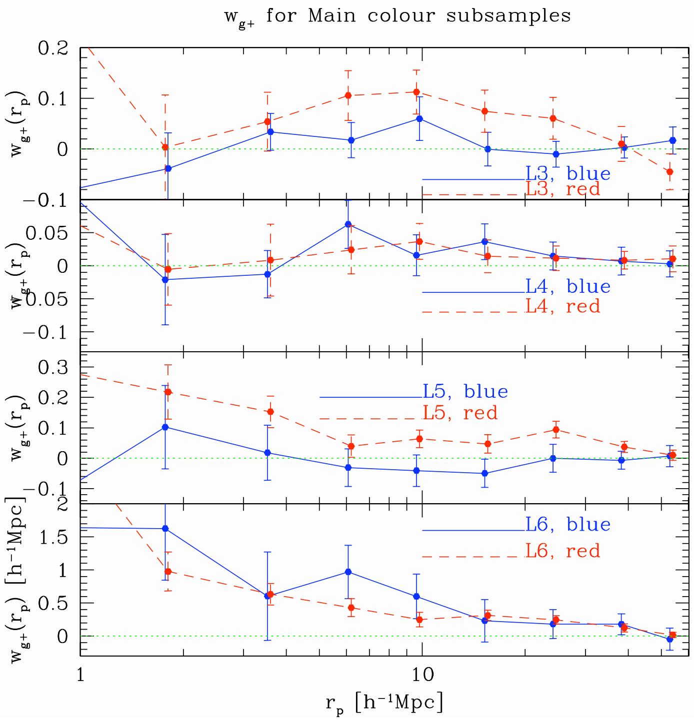

w_g+ for Main colour subsamples
L3, blue
L3, red
L4, blue
L4, red
L5, blue
L5, red
L6, blue
L6, red
w_g+(r_p)
w_g+(r_p) [h^-1Mpc]
r_p [h^-1Mpc]

Non-linear structure formation

Problems

- Non-linear predictions of dark-matter P_δ not better than $\approx 5\%$ on small scales [Peacock&Dodds 1996, Smith, Peacock et al. 2003]
- With baryonic physics much worse!
- Dark energy dependence not really tested, extrapolations valid?
- Accuracy of non-linear bispectrum B_δ $15 - 30\%$ [Scoccimarro & Couchman 2001]
- Halo model, semi-analytic, works also for higher-order statistics, but many fine-tuning parameters

Necessary accuracy of P_δ not to be dominated by systematic errors in P_δ (@ $k \sim 1$ h/Mpc).

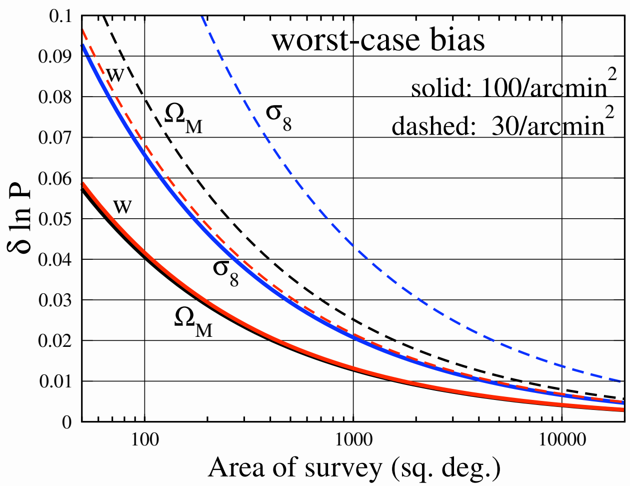

[Huterer & Takada 2005]

Non-Gaussian errors

- Second-order correlations

$$\langle \varepsilon_i \varepsilon_j^* \rangle = \langle \varepsilon_i^{\rm s} \varepsilon_j^{\rm s*} \rangle + \langle \gamma_i \gamma_j^* \rangle = \sigma_\varepsilon^2 \delta_{ij} + \xi_+(\vartheta_{ij})$$

- Error of second-order correlations is square of above. Schematically:

$$\begin{aligned} \mathrm{cov} &= c_1\, \sigma_\varepsilon^4 + c_2\, \sigma_\varepsilon^2 \, \langle \gamma\gamma \rangle + c_3 \, \langle \gamma\gamma\gamma\gamma \rangle \\ &\equiv D + M + V \end{aligned}$$

D : 'diagonal term', shot noise due to intrinsic ellipticity and finite numbers of galaxies

M : mixed term

V : sample "cosmic" variance, due to finite observed volume

Cosmic variance term V

If shear field were Gaussian: $V = 3 \langle \gamma\gamma \rangle^2$, cov known analytically [Schneider, van Waerbeke, MK & Mellier]. But this is not the case! What is $\langle \gamma\gamma\gamma\gamma \rangle_c$?

Possible ways to get $V_{\rm non-Gauss}$:

- Field-to-field variance from data, if large number of independent patches observed
- From ray-tracing simulations
- Fitting formulae [Semboloni et al. 2007]
- Cov. of P_κ, fourth-order statistics from halo-model, [e.g. Cooray & Hu 2001]

Covariance for CFHTLS Wide, 55 $\deg^2$

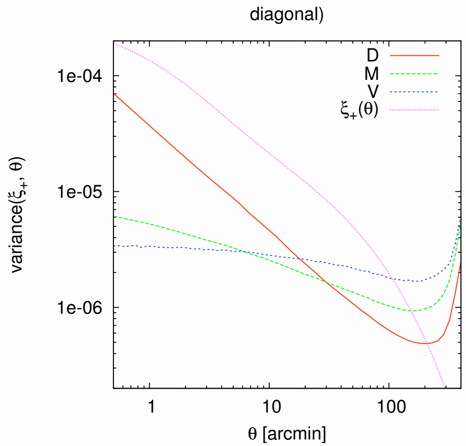

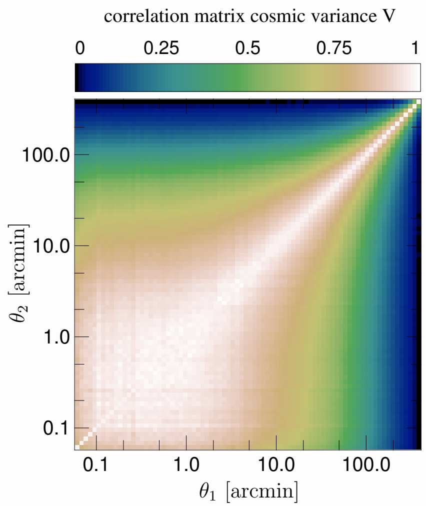

Non-Gaussian cosmic variance important on small scales

$\langle M_{\rm ap}^2 \rangle$, survey area = 3 square degree

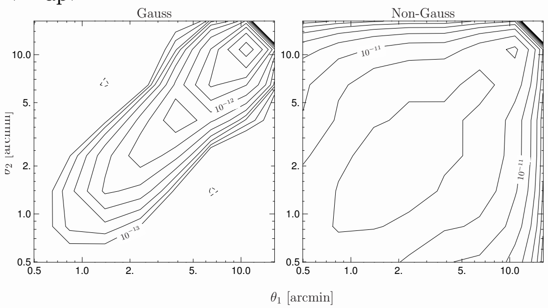

[MK & Schneider 2005]

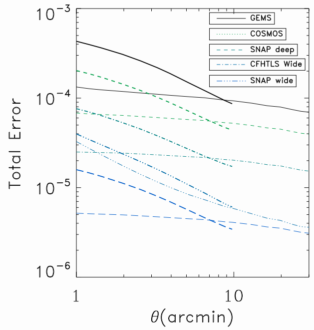

[Semboloni et al. 2007]

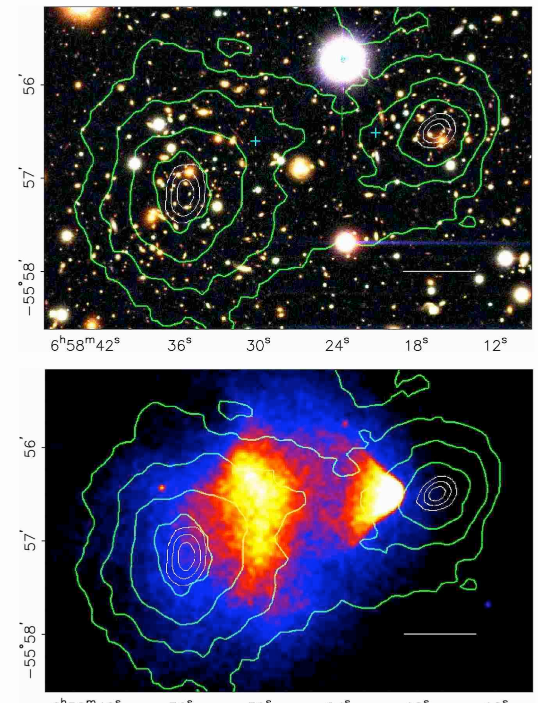
56'
57'
−55°58'
6h58m42s
36s
30s
24s
18s
12s

Results from the bullet cluster

- Combined strong+weak lensing, optical, X-ray analysis [Bradač et al., Clowe et al. 2006]
- Self-interaction of dark matter: $\sigma/m < 1.25\text{cm g}^{-1}$ [Randall et al. 2007]
- [Angus, Shan, Zhao & Famaey 2007]: MOND + 2 eV hot neutrinos as collisionless dark matter, falsifiable by KATRIN β-decay experiment by 2009. Not a new idea [Sanders 2003, McGaugh 2004]

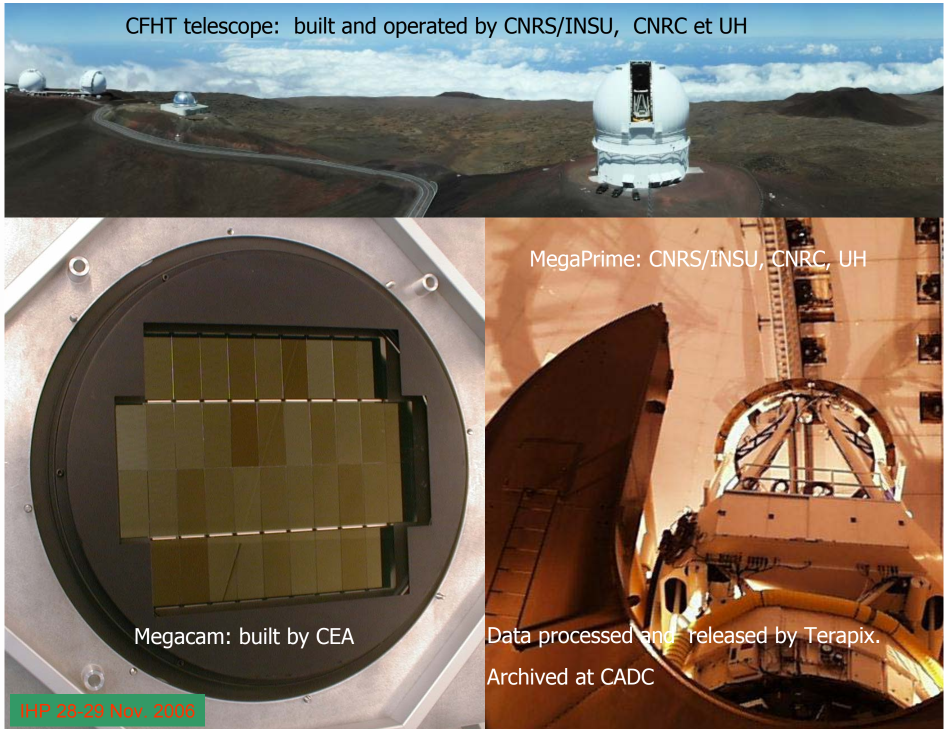
CFHT telescope: built and operated by CNRS/INSU, CNRC et UH
MegaPrime: CNRS/INSU, CNRC, UH
Megacam: built by CEA
Data processed and released by Terapix.
Archived at CADC
IHP 28-29 Nov. 2006

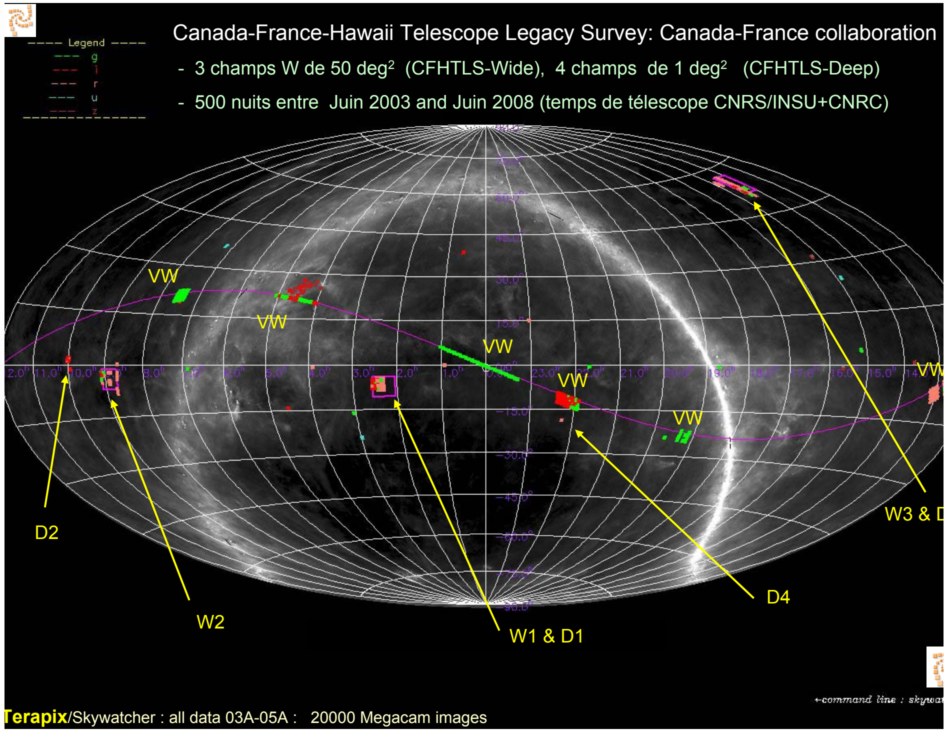
Canada-France-Hawaii Telescope Legacy Survey: Canada-France collaboration
- 3 champs W de 50 deg² (CFHTLS-Wide), 4 champs de 1 deg² (CFHTLS-Deep)
- 500 nuits entre Juin 2003 and Juin 2008 (temps de télescope CNRS/INSU+CNRC)
Legend
VW
VW
VW
VW
VW
VW
D2
W2
W1 & D1
D4
W3 & D
Terapix/Skywatcher : all data 03A-05A : 20000 Megacam images

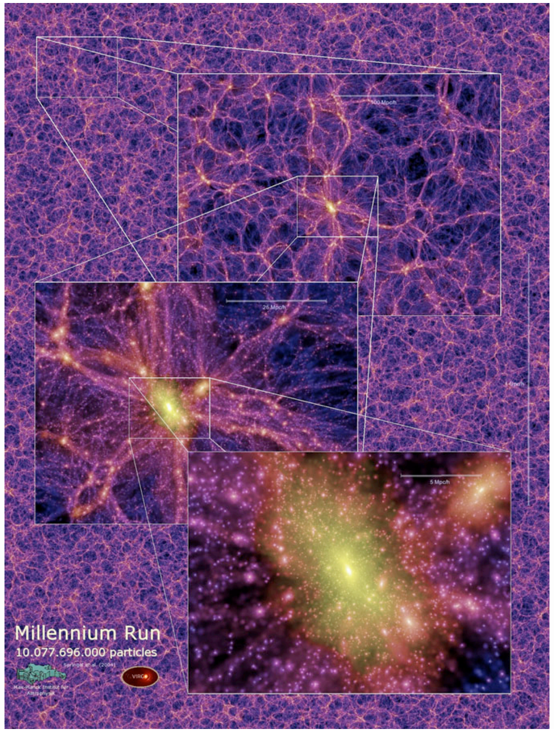
Millennium Run
10.077.696.000 particles

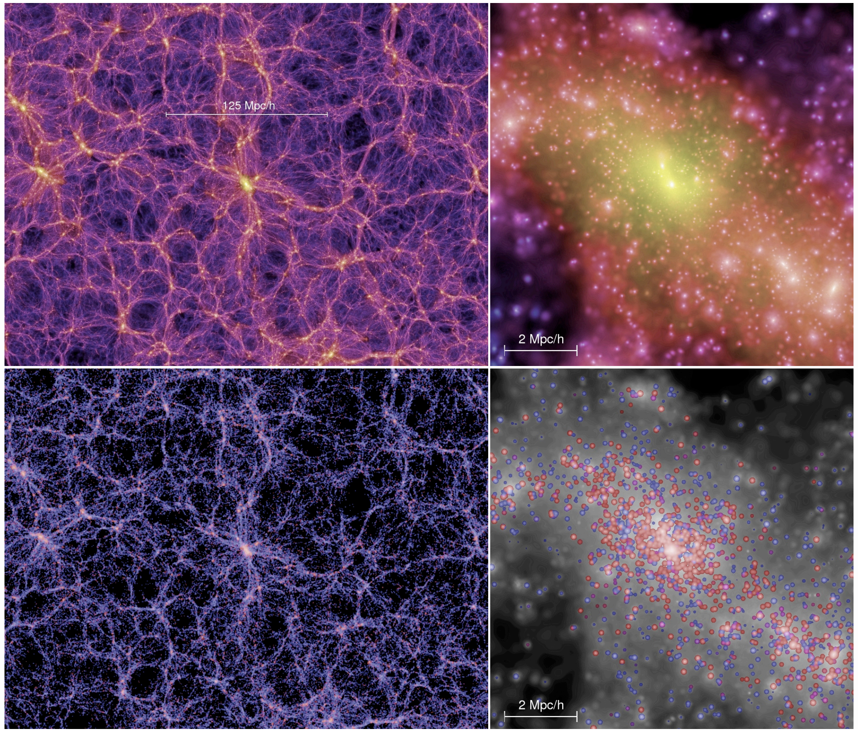

125 Mpc/h
2 Mpc/h
2 Mpc/h